AD-A186 667 O2-I LASER (OXYGEN-IODINE) MIXING STUDIES USING LIF (LASER INDUCED FLUORESCENCE)(U) AIR FORCE WEAPONS LAB KIRTLAND AFB NM Y D JONES ET AL. JUL 87 AFWL-TR-86-119 1/1

UNCLASSIFIED F/G 9/3 NL

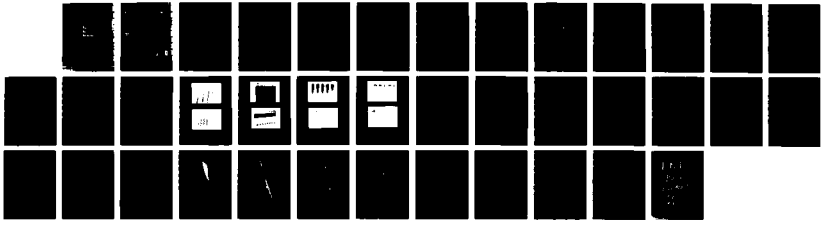

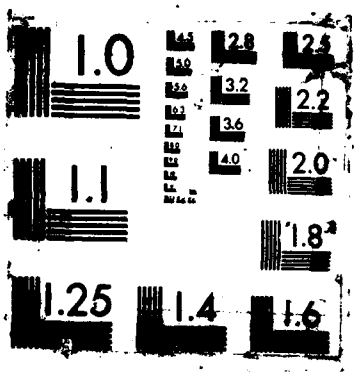
1.0
1.1
1.25
1.4
1.6
1.8
2.0
2.2
2.5
2.8
3.2
3.6
4.0

AFWL-TR-
86-119

O_2-I LASER MIXING STUDIES USING LIF

Y. D. Jones
D. Plummer
L. J. Watkins
G. D. Hager

July 1987

Final Report

Approved for public release; distribution unlimited.

AIR FORCE WEAPONS LABORATORY
Air Force Systems Command
Kirtland Air Force Base, NM 87117-6008

This final report was prepared by the Air Force Weapons Laboratory, Kirtland Air Force Base, New Mexico, Job Order 33261U01. Dr. Yolanda D. Jones (AWYW) was the Laboratory Project Officer-in-Charge.

When Government drawings, specifications, or other data are used for any purpose other than in connection with a definitely Government-related procurement, the United States Government incurs no responsibility or any obligation whatsoever. The fact that the Government may have formulated or in any way supplied the said drawings, specifications, or other data, is not to be regarded by implication, or otherwise in any manner construed, as licensing the holder, or any other person or corporation; or as conveying any rights or permission to manufacture, use, or sell any patented invention that may in any way be related thereto.

This report has been authored by employees of the United States Government. Accordingly, the United States government retains a nonexclusive, royalty-free license to publish or reproduce the material contained herein, or allow others to do so, for the United States Government purposes.

This report has been reviewed by the Public Affairs Office and is releasable to the National Technical Information Service (NTIS). At NTIS, it will be available to the general public, including foreign nations.

If your address has changed, if you wish to be removed from our mailing list, or if your organization no longer employs the addressee, please notify AFWL/AWYW Kirtland Air Force Base, NM 87117-6008 to help us maintain a current mailing list.

This report has been reviewed and is approved for publication.

Yolanda D. Jones

YOLANDA D. JONES, PhD
Project Officer

FOR THE COMMANDER

Gerald A Hasen

GERALD A. HASEN
Maj, USAF
Ch, Advanced Chemical Laser Branch

HARRO ACKERMANN
Lt Col, USAF
Ch, Laser Science Technology Office

DO NOT RETURN COPIES OF THIS REPORT UNLESS CONTRACTUAL OBLIGATIONS OR NOTICE ON A SPECIFIC DOCUMENT REQUIRES THAT IT BE RETURNED.

UNCLASSIFIED
SECURITY CLASSIFICATION OF THIS PAGE

REPORT DOCUMENTATION PAGE

1a. REPORT SECURITY CLASSIFICATION Unclassified	1b. RESTRICTIVE MARKINGS
2a. SECURITY CLASSIFICATION AUTHORITY	3. DISTRIBUTION / AVAILABILITY OF REPORT Approved for public release; distribution unlimited.
2b. DECLASSIFICATION / DOWNGRADING SCHEDULE	
4. PERFORMING ORGANIZATION REPORT NUMBER(S) AFWL-TR-86-119	5. MONITORING ORGANIZATION REPORT NUMBER(S)
6a. NAME OF PERFORMING ORGANIZATION Air Force Weapons Laboratory 6b. OFFICE SYMBOL (If applicable) AWYW	7a. NAME OF MONITORING ORGANIZATION
6c. ADDRESS (City, State, and ZIP Code) Kirtland Air Force Base, NM 87117-6008	7b. ADDRESS (City, State, and ZIP Code)
8a. NAME OF FUNDING / SPONSORING ORGANIZATION 8b. OFFICE SYMBOL (If applicable)	9. PROCUREMENT INSTRUMENT IDENTIFICATION NUMBER
8c. ADDRESS (City, State, and ZIP Code)	10. SOURCE OF FUNDING NUMBERS PROGRAM ELEMENT NO. 62601F; PROJECT NO. 3326; TASK NO. 1U; WORK UNIT ACCESSION NO. 01

11. TITLE (Include Security Classification)
O_2-I LASER MIXING STUDIES USING LIF

12. PERSONAL AUTHOR(S)
Jones, Y.D.; Plummer, D.; Watkins, L.J.; Hager, G.D.

13a. TYPE OF REPORT	13b. TIME COVERED	14. DATE OF REPORT (Year, Month, Day)	15. PAGE COUNT
Final	FROM Jan 83 TO Jan 85	1987 July	38

16. SUPPLEMENTARY NOTATION

17. COSATI CODES		
FIELD	GROUP	SUB-GROUP
09	03	

18. SUBJECT TERMS (Continue on reverse if necessary and identify by block number)
Oxygen-iodine, Laser induced fluorescence, Nozzle, Fluid dynamics, Subsonic mixing.

19. ABSTRACT (Continue on reverse if necessary and identify by block number)

Laser-Induced Fluorescence (LIF) was incorporated to study the degree of mixing in two subsonic nozzle variations for the O_2^n-I laser system. The studies were performed using a testbed version of COIL-IV, an O_2^n-I laser. I_2^n was injected through the nozzles and excited with an $Ar_{\downarrow}^{+}$ laser to produce fluorescence. The observed jet trajectories could then be compared to trajectories predicted by computer models. Velocity distributions were measured at several flow rates. The LIF allowed for an evaluation of the relative degree of mixing produced by the two nozzles resulting in a modification of the O_2^n-I laser.

(Kazuo d:

20. DISTRIBUTION / AVAILABILITY OF ABSTRACT	21. ABSTRACT SECURITY CLASSIFICATION
☒ UNCLASSIFIED/UNLIMITED ☐ SAME AS RPT ☐ DTIC USERS	Unclassified
22a. NAME OF RESPONSIBLE INDIVIDUAL Dr. Yolanda Jones	22b. TELEPHONE (Include Area Code) (505) 844-1871
	22c. OFFICE SYMBOL AFWL/AWYW

DD FORM 1473, 84 MAR — 83 APR edition may be used until exhausted. All other editions are obsolete.

SECURITY CLASSIFICATION OF THIS PAGE
UNCLASSIFIED

CONTENTS

ILLUSTRATIONS

I. INTRODUCTION

The following experiments and analyses were designed to examine and understand the level of mixing present in an existing O_2-I laser - COIL-IV. The O_2-I laser did not originally demonstrate gain and power at the levels predicted by theory. Gain was also seen to increase with secondary flow rate. One possible answer was insufficient mixing of the secondary stream (I_2 and diluent) into the primary stream of O_2.

Since the O_2-I laser system depends upon a diffusion-limited process to dissociate the I_2 into I-atoms and then to excite the I-atoms, mixing is an extremely critical parameter. Mixing is dependent upon factors such as the momentum match of the input flows and jet trajectory and poses a complex problem for study. To better understand the momentum match of the primary and secondary flows in COIL-IV, as well as, to examine trajectories and mixing capabilities of the I_2 injectors, a sectional unit (ReCOIL) was developed for cold flow experiments and constructed to accommodate diagnostics to be used in quantifying flow conditions.

The flow from the injectors into the primary flow was examined by laser-induced fluorescence (LIF) of iodine seeded into the secondary flow. The excitation laser beam was manipulated to illuminate a single plane or a variable sized section in the cavity. Two types of nozzles were investigated. The first (Nozzle No. 1) was the nozzle originally used in COIL-IV. Nozzle No. 2 contained more orifices and different injection angles. The LIF information is compared to jet trajectory theory in an effort to determine the accuracy of the theoretical approach. Information gathered from the ReCOIL testing was incorporated in designing nozzles for COIL-IV to achieve higher small signal gain.

II. APPARATUS

The ReCOIL system was approximately a 1/16th scale of COIL-IV in terms of flow rates. The test-bed contained a cavity section similar to the original laser. Figure 1 shows ReCOIL and associated flow systems. Figures 2a and b contain diagrams of the nozzle types. Nozzle No. 1 contains 7 orifices per injector and 20 injectors centered 1.27 cm apart. Each orifice has a diameter of 0.08 cm. Nozzle No. 2 contains 38 orifices of 0.058-cm-dia and 20 injectors with separations of 1.27 cm.

A Plexiglas cavity was used to allow photographs of the fluorescence to be taken. The cavity was equipped with variable flow directors, or shrouds, also of Plexiglas. All gas lines carrying I_2, including the injectors, were heated to greater than 71^{o}C. Either N_2 or He could be used as the I_2 carrier gas. All fabricated critical orifices were calibrated against a manufacturer calibrated orifice. Pressure transducers and mechanical pressure gauges were positioned upstream and downstream of each orifice to determine gas flow rates and maintain a sonic condition at the orifice. An absorption cell in the I_2 flow system was used to determine the I_2 flow rate. The pressures in the cavity and absorption cell were measured using transducers and the cell and cavity temperatures are measured by thermocouple. The pumping rate and gas flow rates were adjusted to simulate COIL-IV operating conditions.

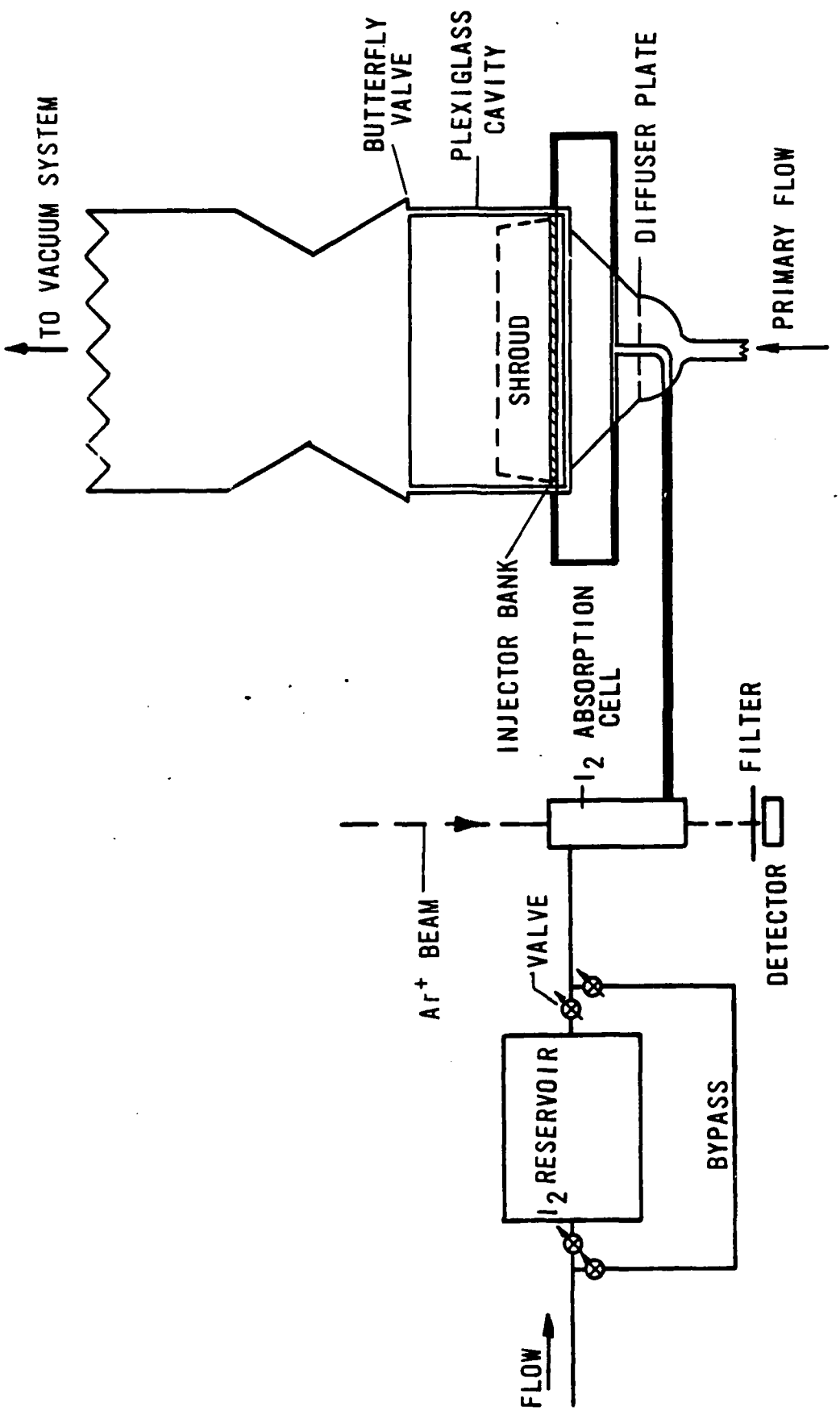

Figure 1. Schematic of test assembly.

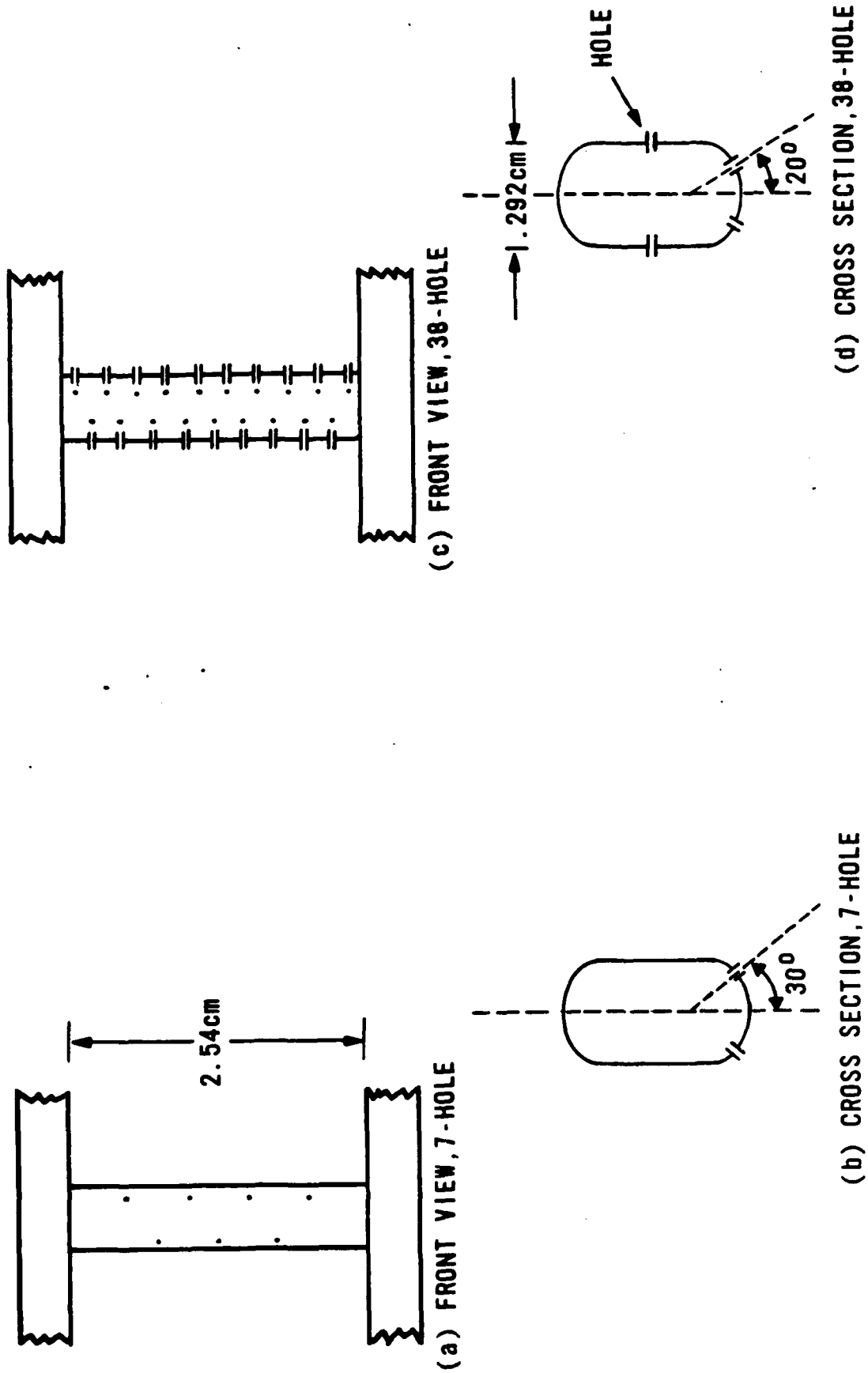

Figure 2. Nozzle section diagrams.

III. DIAGNOSTICS

Several diagnostics were used in conjunction with ReCOIL including LIF, iodine measurement by molecular absorption, and Pitot tube measurement of the flow velocity.

1. LASER-INDUCED FLUORESCENCE METHOD FOR EXAMINING NOZZLE PERFORMANCE

The LIF is a flexible diagnostic tool to observe jet trajectory and mixing in a flow field. The LIF technique is particularly well suited to O_2-I laser mixing analysis since I_2 is normally injected through the nozzles during its operation. The technique is possible due to a match between the strong $I_2(X^1\Sigma, v'' = 0 \rightarrow B^3\pi_0, v' = 43)$ absorption and the 5145 Å line of the Ar^+ laser. The lifetimes of the $B^3\pi_0$, $v' = 43$ and nearby vibrational states are on the order of microseconds. In fact, the technique has been successfully applied to supersonic flow fields because of these short lifetimes. This application involved subsonic flow, thus eliminating any distortion because of the emission lifetime and thus, allowing for good spatial resolution in the study.

A diagram of the experimental arrangement is presented in Figure 3. An Ar^+ laser (Spectra Physics, Model 164) was operated at maximum power in multiline mode and the beam directed onto a high-power grating (Phase-R) for separation of the laser lines. Following the method of Davis and Rapagnani (Ref. 1), the 5145 Å line of the argon-ion laser was directed through the cavity parallel to the plane of the nozzle bank face (in the xy or the xz plane). A raster unit (General Scanning) and cylindrical lens were incorporated to position the laser beam in the cavity and produce a thin sheet of laser light, which was used to examine a single row of orifices and the corresponding mixing. The sheet of light could also be manipulated to run perpendicular to the primary flow (in the xz plane).

The Plexiglas cavity allowed for photographs to be taken from both the top (with the sheet of light in the xy plane) and from the front (sheet in xz plane). The photographs from the front of the cavity were taken at an

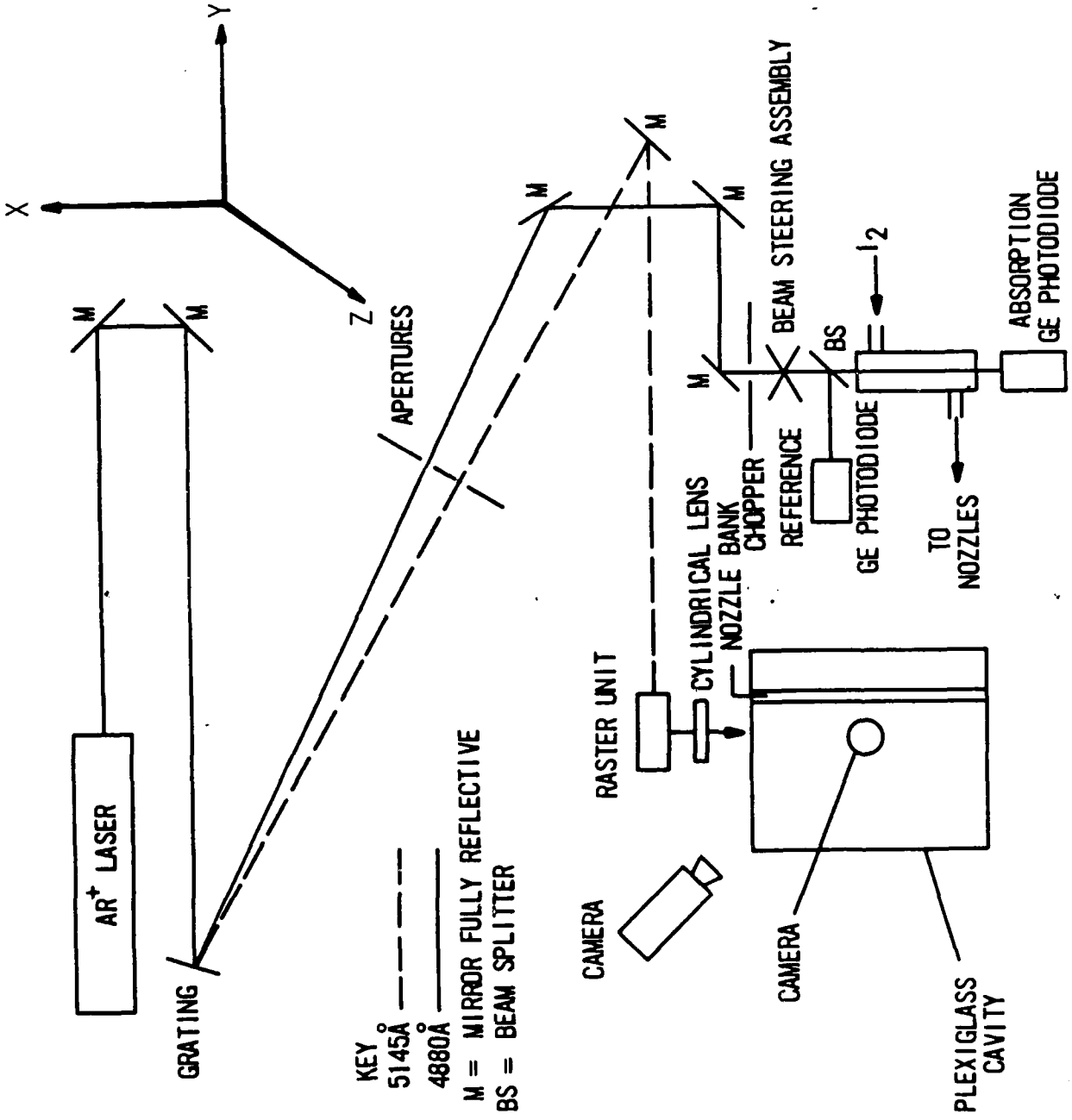

Figure 3. I_2 flow rate and LIF schematic.

oblique angle to the flow (Fig. 3) creating a slight distortion in the photograph. The view field from the top was from the nozzle exit plane (NEP) to 4 cm downstream. The front photographs were taken with the beam positioned at 2 cm downstream from the nozzle exit plane.

Photography was performed using high-speed Polaroid film Type 107 (ASA 3000) and Type 612 (ASA 20,000 equivalent). Some of the photographs are misleading as to the development of mixing due to variations in I_2 concentration (thus emission intensity) and exposure time. It should be noted that visual examination of the mixing was used in conjunction with photography; since the slightly oblique angle required for the camera to photograph the IF in the xz plane caused some distortion.

2. I_2 FLOW RATE DETERMINATION

The I_2 flow rate was a critical parameter in calculating the momentum of the jet. The I_2 delivery system was subject to large variations in flow rate. It was, therefore, important to use a real time measurement. The ratio of I_2 to primary flow rate was adjusted to approximate conditions, and thus momentum, in the O_2-I laser system. The method for I_2 flow rate determination has been previously described in Reference 2. Before entering the injectors, the secondary flow is directed through a heated 10 cm absorption cell. Cell pressure was monitored using a MKS Baratron pressure transducer (0-100 torr) and temperature was measured using a thermocouple. The general optical arrangement used is shown in Figure 3. The 4880 Å beam from the grating (LIF Method section) was directed through the cell for direct measurement of the I_2 concentration by resonance absorption.

The Ge photodiodes were used for reference and absorption signal detection. The 4880 Å beam was chopped, with the signals from the photodiodes being fed into lock-in amplifiers and ultimately into a ratiometer (PAR Model 5101 and Model 188, respectively). The I_2 concentration was then calculated from the absorption using the known cross section.

3. VELOCITY MEASUREMENTS

To determine the velocity profile across the cavity, a Pitot tube (0.318-cm-dia) was used to vertically scan the face of the nozzles. The tip of the Pitot was approximately 8.89 cm downstream of the nozzle. The static pressure was measured at the top of the cavity. Both measurements were performed using pressure transducers (MKS Baratron, 0-10 torr). Only high flow rate conditions were measured due to (a) the lack of sensitivity of the pressure measurements at low flow rates, and (b) the decreasing dependence of pressure ratio an Mach number at low Mach number. Most measurements were performed in subsonic flow corresponding to the O_2-I laser conditions.

The relationship of pressure ratio to Mach number under subsonic flow conditions is described by:

$$\frac{P_o}{P} = \left(\frac{1 + \frac{\gamma-1}{2} M^2}{}\right)^{\gamma/\gamma-1} \qquad (1)$$

where

P_o = Pitot tube pressure

P = static pressure

$\gamma = C_p/C_v$

M = Mach number

Calculation of the velocity and Mach number from the flow rates and cavity pressures have indicated that the centerline most closely approximates the predicted values. This is mainly due to the lack of sensitivity of this method at low Mach number (< 0.2). The wall areas of the cavity cause drag which decreases the velocity as shown at the top and bottom of the profile.

4. CALIBRATION OF THE FLOW SYSTEM

The flow rates of all of the gases are critical parameters in determining compliance of jet trajectory theory to experiment. It was, therefore, important to carefully determine the gas flow rates. Manufactured sonic orifices were often used (Flowdyne) which were calibrated for several gases. The upstream and downstream pressures of the orifice were monitored to ensure a sonic condition and to calculate flow rates. Often, orifices were fabricated on-site. In the case of a fabricated critical orifice, the calibration was achieved by setting specific flow rates with a calibrated orifice and ensuring a sonic condition existed at both orifices. The known flow rate was correlated to measured upstream pressures for the uncalibrated orifice yielding a calibration of the fabricated orifice for the specific gas employed.

All pressure measurement instruments were calibrated with either a McLeod gauge or an Heise gauge. Periodic calibrations were performed to ensure consistency and accuracy. Pumping curves were determined to ensure that conditions were equivalent to COIL-IV.

IV. EXPERIMENTAL RESULTS

1. LASER-INDUCED FLUORESCENCE

Experimental flow rates were equivalent to 1/16th the flow rates used in COIL-IV. The N_2 was used in place of O_2 for primary flow and either He or N_2 was used as the secondary (or carrier) flow. The primary flow was set at the 0.5 or 1.0 moles/s equivalent in COIL-IV. For the 0.5 mole/s equivalent (0.03 moles/s), the carrier was run at 0.009, 0.015, 0.0215, and 0.030 moles/s. In the 1.0 mole/s equivalent case (0.06 moles/s), all secondary flows were doubled to achieve momentum matched flow conditions. Under each set of conditions, the I_2 flow rate remained between 0.5 to 1.0 percent of the primary flow rate.

Samples of the photographic documentation are shown in Figures 4 through 7. Table 1 details the flow rates and other pertinent conditions for each photograph.

As mentioned earlier, gain in the O_2-I laser was soon to be sensitive to changes in the secondary flow (Fig. 8). As can be seen in Figures 4 through 7, mixing is also quite sensitive to this parameter. A comparison of the mixing performance to the gain curves implicate the improved mixing is responsible for improved gain.

As a result, Nozzle No. 2 was designed with a finer injection scale. Nozzle No. 2 had more developed mixing and thus better I_2 distribution. Best mixing occurred at high carrier flows, with N_2 yielding better mixing than He at the same molar flow rate. This is considered to be partly an increased momentum effect due to the higher molecular weight of N_2; however, the higher pressures required for N_2 to achieve the same molar flow rate as He caused a higher pressure in the generator of the O_2-I laser. Therefore, a compromise between better mixing and increased generator pressures had to be reached in COIL-IV operation.

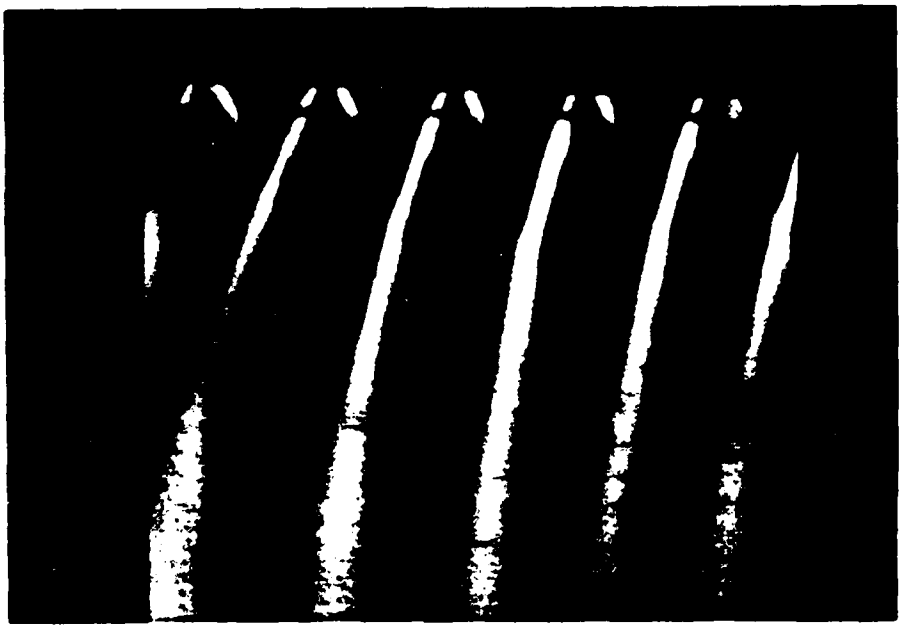

(a) Top view

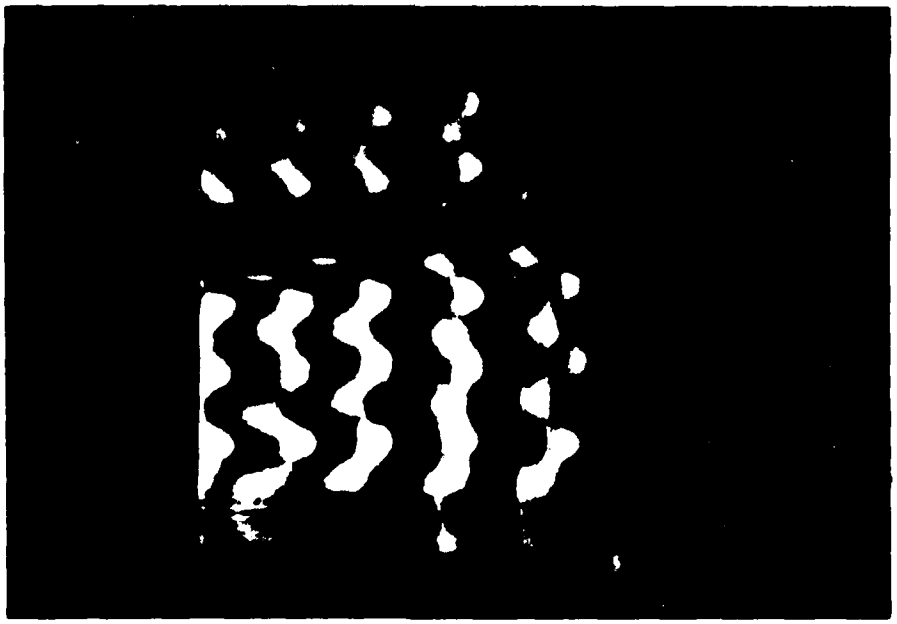

(b) Front view

Figure 4. LIF with $\dot{m}_{He} = 2.64 \times 10^{-2}$ moles/s using Nozzle No. 1.

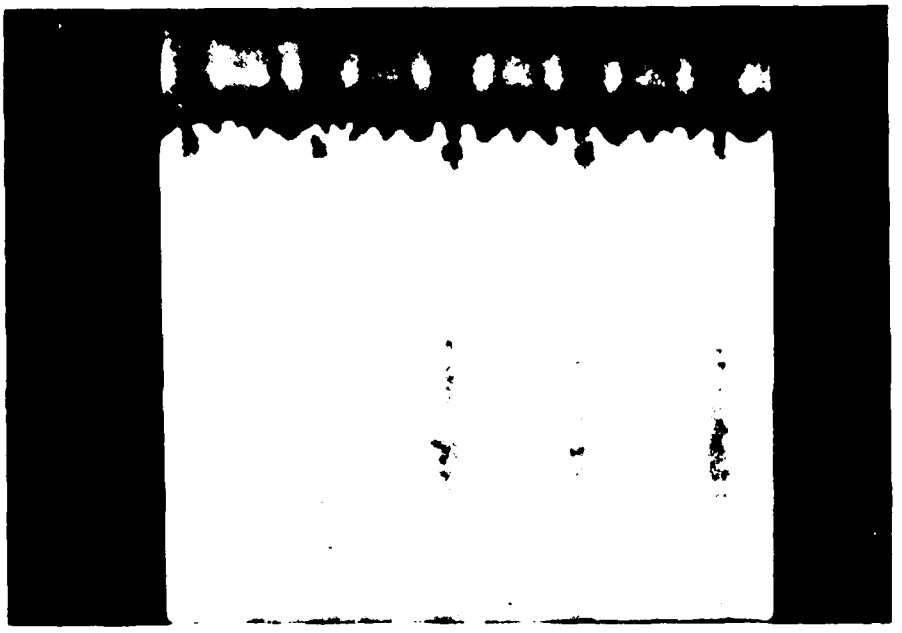

(a) Top view

(b) Front view

Figure 5. LIF with (a) $\dot{m}_{N_2} = 2.64 \times 10^{-2}$ moles/s using Nozzle No. 2.

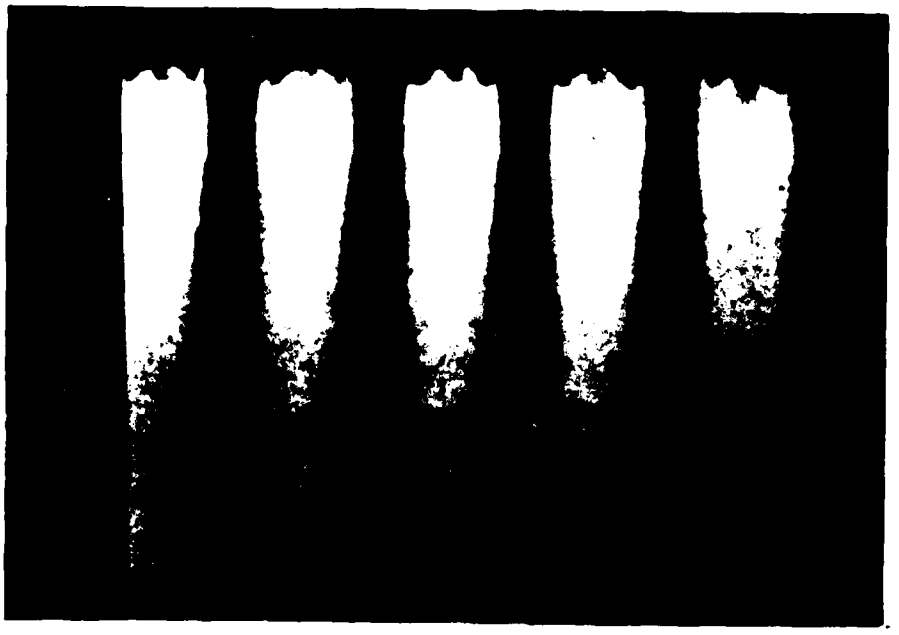

(a)

(b)

Figure 6. (a) LIF with $\dot{m}_{N_2} = 8.90 \times 10^{-3}$ moles/s.
(b) $\dot{m}_{N_2} = 1.78 \times 10^{-2}$ moles/s.

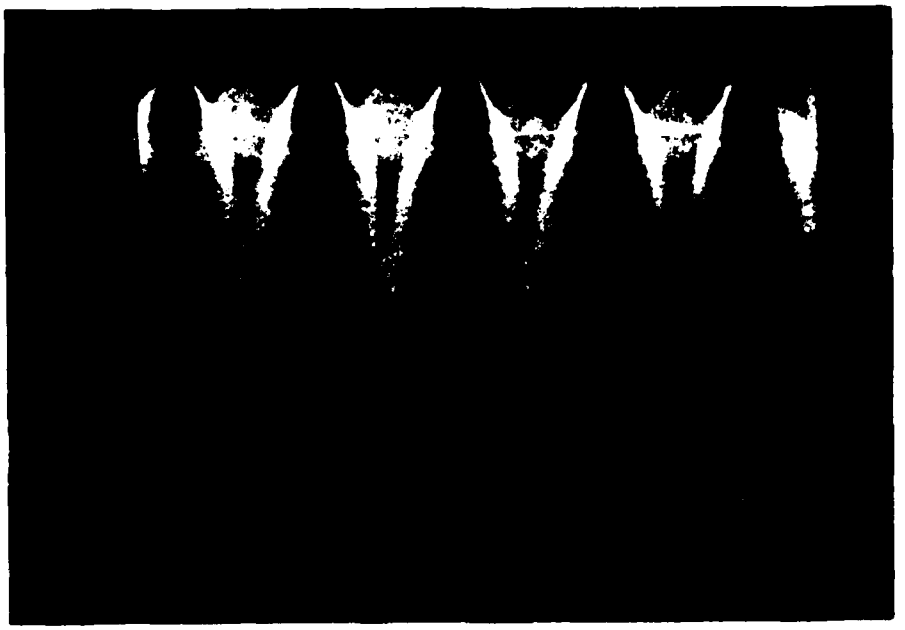

(a)

(b)

Figure 7. (a) LIF with $\dot{m}_{N_2} = 2.64 \times 10^{-2}$ moles/s.

(b) $\dot{m}_{N_2} = 3.52 \times 10^{-2}$ moles/s.

TABLE 1. LIF PHOTOGRAPH FLOW CONDITIONS

Nozzle No.	Primary $\dot{m}_{N_2}$ (moles/s)	Secondary $\dot{m}_{He}$ or $\dot{m}_{N_2}$ (moles/s)	$\dot{m}_{I_2}$ (moles/s)	P_{cav} (torr)[a]	P_{cell} (torr)[a]	T_{cell} (°C)	Figure No.
1	0.06	2.64×10^{-2} He	4.89×10^{-4}	4.27	33.8	102.2	4a, b
2	0.06	2.64×10^{-2} He	4.05×10^{-4}	4.37	41.6	95.6	5a, b
2	0.06	8.90×10^{-3} N_2	5.35×10^{-4}	3.28	11.1	91.7	6a
2	0.06	1.78×10^{-2} N_2	6.97×10^{-4}	3.48	16.7	92.2	6b
2	0.06	2.64×10^{-2} N_2	3.34×10^{-4}	4.84	52.1	92.8	7a
2	0.06	3.52×10^{-2} N_2	5.06×10^{-4}	4.51	44.4	93.3	7b

[a] 1 torr = 1.33×10^2 Pascal

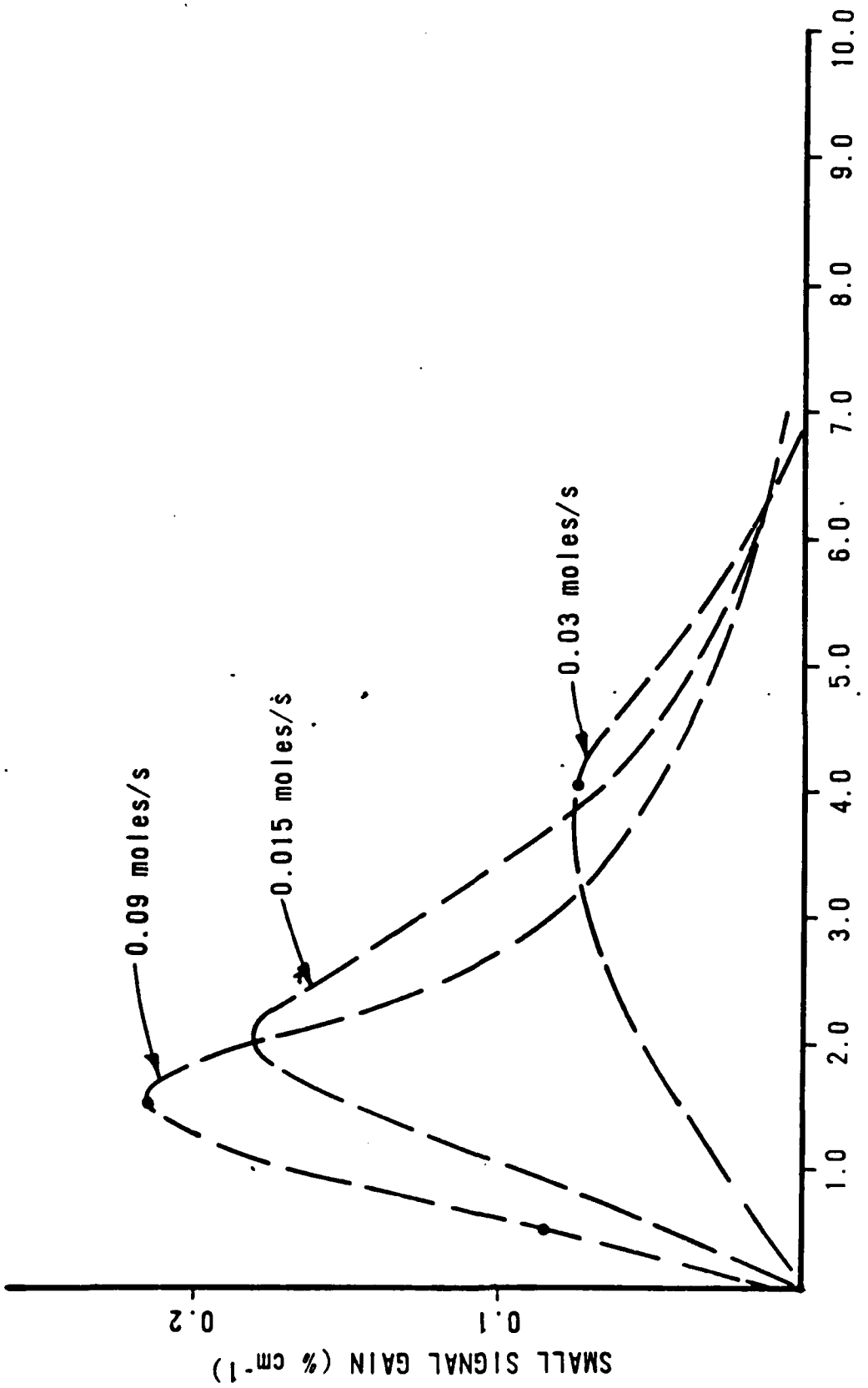

Figure 8. SSG dependence on secondary flow rate.

2. VELOCITY PROFILES

Figures 9a and b contain sample profiles of the velocity measurements performed. Figures 9a and b are both subsonic conditions. Figure 9a shows a profile with Nozzle No. 2, the N_2 primary flow rate at 0.06 moles/s and N_2 secondary flow rate at 0.0352 moles/s. Figure 9b was taken at the same flow rates but with He secondary. The butterfly valve (Fig. 1) was slightly closed as well. The deviation from the classic parabolic shape is due to the insensitivity of the diagnostic system at low pressure differences (low Mach number) near the shrouds. Therefore, the centerline measurements are more accurate.

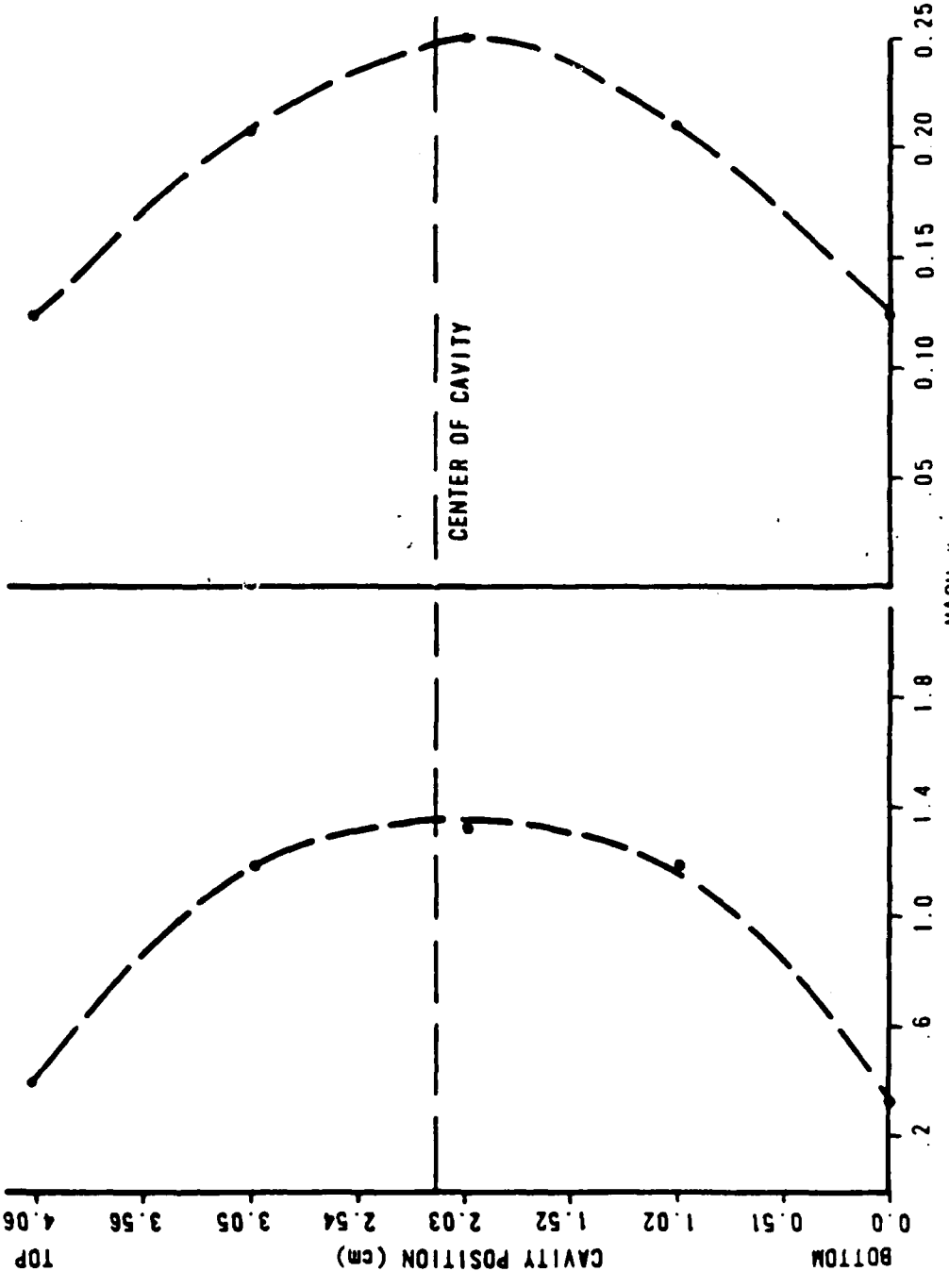

(a) With N_2 secondary (b) With He Secondary

Figure 9. Sample velocity profiles with different secondary carrier gas.

V. ANALYTICAL RESULTS

Besides evaluating overall mixing with the nozzles in a qualitative manner, the purpose of the LIF studies also included: (a) to determine the trajectory for a secondary flow, inclined at some arbitary angle to the primary flow, and (b) to compare these results with a model of the jet trajectory. The following discussion will detail the model of the jet trajectories and compare the results of the experimental data against this model.

The technique presented here for predicting jet trajectories from a sonic orifice into subsonic flow follows the approach presented by Schetz and Billig (Ref. 3) for gaseous jets injected into supersonic flow. To proceed with the prediction of a general jet trajectory one must first ascertain which of two types of jets, pressure matching or underexpanded, is present. This depends on the magnitude of the parameter P_j/P_∞ where P_j is the static pressure in the jet at the orifice exit and P_∞ is the free-stream static pressure. For values of $P_j/P_\infty < 2$, a pressure matching jet which issues smoothly from orifice exists and its trajectory can be calculated from Ivanov (Ref. 4):

$$\frac{x}{d} = \left(\frac{q_{01}}{q_{02}}\right)^{1.3} \left(\frac{y}{d}\right)^3 + \frac{y}{d} \cot \alpha \qquad (2)$$

where x and y are the coordinates of the centerline points of the jet (Fig. 10); d is the diameter of the orifice and α is the angle between the direction of the axis of the orifice and the direction of the deflecting flow. The q_{01} and q_{02} are the dynamic pressures in the free stream and in the jet's initial cross-section, respectively, and are given by:

$$q_{01} = \rho_1 \frac{w^2}{2} \qquad (3)$$

$$q_{02} = \rho_2 \frac{v_o^2}{2} \qquad (4)$$

$$\frac{(X - X_m \cos \alpha_0)}{D} = \left(\frac{q_{01}}{q_{02}}\right)^{1.3} \left(\frac{y - X_m \sin \alpha_0}{D}\right)^3 + \frac{(y - X_m \sin \alpha_0) \cot X_0}{D}$$

WHERE q_{02} IS NOW CALCULATED FROM CONDITIONS DOWNSTREAM OF THE MACH DISK BY

$$q_{02} = \frac{P_2 \gamma m_2^2}{2}$$

AND

$$D = \sqrt{\frac{4m_j}{\pi \rho_2 V_2}}$$

$$\frac{X_m}{d} = .632 \sqrt{\frac{P_0}{P_\infty}}$$

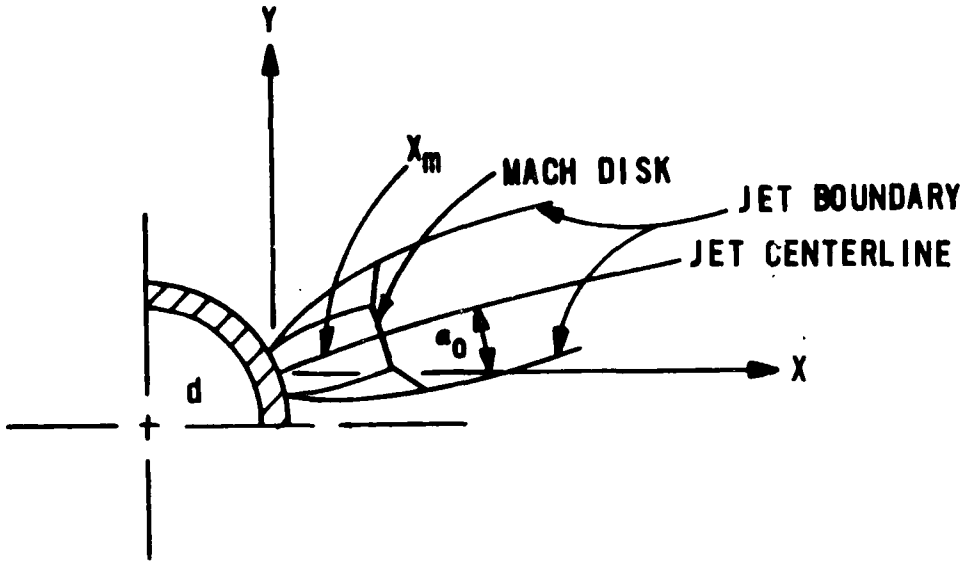

Figure 10. Jet trajectory analysis.

For values of $P_j/P_\infty > 2$, an underexpanded jet is formed as depicted in Figure 10. From the experimental data, it is clear that the nozzle injection conditions resulted in underexpanded jets. The underexpanded jet is characterized by a normal shock Mach Disk of a diameter D_m, at a distance X_m, downstream of the orifice. The flow upstream of the Mach Disk is supersonic and that downstream is subsonic. To determine the trajectory of this type of jet the following assumptions are made:

a. The position of the Mach Disk remains directly on the orifice centerline regardless of the free stream velocity;

b. The Ivanov trajectory relationship is valid with the jet momentum determined from conditions downstream of the Mach Disk; and,

c. The static pressure downstream of the Mach Disk is equal to the primary free stream static pressure.

With these assumptions, the underexpanded jet trajectory from an orifice at angle α_o to the free stream (Fig. 10) is given by Equation 2. If the x and y axis is translated by the distance X_m, and multiplied by the appropriate trigonometric function Equation 5 results.

$$\frac{(x-X_m \cos \alpha_o)}{d} = \left(\frac{q_{01}}{q_{02}}\right)^{1.3} \left(\frac{y-X_m \sin \alpha_o}{d}\right)^3 + \frac{(y-X_m \sin \alpha_o) \cot \alpha_o}{d} \qquad (5)$$

where q_{02} is now calculated from conditions downstream of the Mach Disk by:

$$q_{02} = \frac{P_2 \gamma M_2^2}{2} \qquad (6)$$

There is a degree of uncertainty regarding the appropriate diameter, d, to use in Equation 5. The upper limit of the diameter will be D_m, given by:

$$D_m = \sqrt{\frac{4\dot{m}_j}{\pi \rho_2 V_2}} \qquad (7)$$

Equation 7 is generated from mass continuity using the properties downstream of the Mach Disk, where $\dot{m}_j$ is the total mass flow rate through secondary jet.

The upper bound, represented by Equation 7, appears fundamentally more valid than using the orifice diameter and is used for the following analysis.

The position and magnitude of a Mach Disk in front of a sonic orifice have been experimentally determined for a number of gases by Crist (Ref. 5) and Love (Ref. 6). These data have been correlated by the following two expressions for D_m and X_m:

$$\frac{D_m}{d} = 0.316 \sqrt{\frac{P_o}{P_\infty}} \tag{8}$$

$$\frac{X_m}{d} = 0.632 \sqrt{\frac{P_o}{P_\infty}} \tag{9}$$

for

$$P_o/P_\infty > 5 \tag{10}$$

where P_o is the jet stagnation pressure, P_∞ is the free stream ambient pressure surrounding the jet, and d is the sonic orifice diameter.

The conditions downstream of the Mach Disk are determined by iteration of the normal shock relations knowing the jet stagnation pressure and the primary free stream static pressure. An iterative process is then used to determine M_1 and M_2, for use in Equation 6, by comparison to P . This procedure starts by estimating the Mach number upstream of the shock, M_1, from the following expression given in Reference 5:

$$M_1 = \left\{ \frac{X_m}{D_m} \left[\frac{\gamma + 1}{4.8} \left(\frac{\gamma - 1}{2} \right)^{\frac{\gamma}{\gamma - 1}} \right]^{-1/2} \right\}^{\gamma - 1} \tag{11}$$

The Mach number downstream of the Mach Disk is then calculated using:

$$M_2 = \sqrt{\frac{2 + (\gamma-1)M_1^2}{2\gamma M_1^2 - \gamma + 1}} \tag{12}$$

The static pressure, P_2, corresponding to M_2 is given by:

$$P_2 = P_{T1} \times \left(\frac{P_{T2}}{P_{T1}}\right)\left(\frac{P_2}{P_{T2}}\right) \tag{13}$$

where P_{T1} is the pressure upstream of the Mach disk, and assumed to correspond to the nozzle stagnation pressure (P_o) and P_{T2} is the pressure downstream of the Mach disk. P_{T2}/P_{T1} is assumed to be given by:

$$\frac{P_{T2}}{P_{T1}} = \left[\frac{\frac{\gamma+1}{2} M_1^2}{1 + \frac{\gamma-1}{2} M_1^2}\right]^{\frac{\gamma}{\gamma-1}} \left(\frac{2\gamma}{\gamma+1} M_1^2 - \frac{\gamma-1}{\gamma+1}\right)^{\frac{1}{1-\gamma}} \tag{14}$$

and similarly

$$\left(\frac{P_2}{P_{T2}}\right) = \left(1 + \frac{\gamma-1}{2} M_2^2\right)^{\frac{\gamma}{1-\gamma}} \tag{15}$$

P_2 is then compared to P_∞. M_1 is adjusted up or down to enable P_2 to equal P_∞. In a similar manner, knowing T_o, one can evaluate T_2 from the following:

$$T_2 = \left(\frac{T_2}{T_1}\right)\left(\frac{T_1}{T_{T1}}\right) \times T_{T1} \tag{16}$$

where,

$$T_{T1} = T_o \text{ (the stagnation temperature)} \tag{17}$$

and T_1 and T_2 are the static temperatures upstream and downstream of the Mach disk, respectively. Therefore,

$$\left(\frac{T_2}{T_1}\right) = \frac{\left(1 + \frac{\gamma-1}{2} M_1^2\right)\left(\frac{2\gamma}{\gamma-1} M_1^2 - 1\right)}{\frac{(\gamma+1)^2 M_1^2}{2(\gamma-1)}} \tag{18}$$

and

$$\left(\frac{T_1}{T_{T1}}\right) = \left(1 + \frac{\gamma - 1}{2} M_1^2\right)^{-1} \tag{19}$$

Knowing T_2, mass continuity can be applied to the conditions downstream of the Mach Disk to determine the jet diameter using Equation 8.

This procedure was applied to the LIF data. The experimental data requires some qualifications. The data consisted of Polaroid photographs (Fig. 4 for example) showing the secondary jets issuing from the injectors. The outline of selected jet plumes were manually digitized using a graphics digitizer/plotter attached to a computer. It was somewhat difficult to differentiate the boundary of the jets especially when they were several centimeters downstream of the injector. The experimental flow conditions, especially the stagnation pressure associated with the jet, had to be calculated knowing the conditions in a diagnostic cell several feet from the injector manifold. Some error in the calculations may be due to the pressure losses in the I_2 feed line and, therefore, uncertainty in the injection pressure. The resulting comparison of the jet trajectory prediction procedure with data is given in Figures 11 to 14 where several conditions are presented for the two nozzle configurations used.

Figures 11 and 12 present experimental jet plumes for the original COIL-IV (7 hole/injector) nozzle for two values of secondary nitrogen diluent. The theoretical centerline predictions compare quite favorably with the experimental jet trajectory. Small errors may have been introduced from machining irregularities in the injector orifice size and injection angle. Figures 13 and 14 show the comparison of the theoretical jet trajectories versus experimental data for the improved injector indicating the affect of changing secondary diluent from nitrogen to helium. It appears that the theory does not predict the trajectory for the 90 deg jet as well as in the

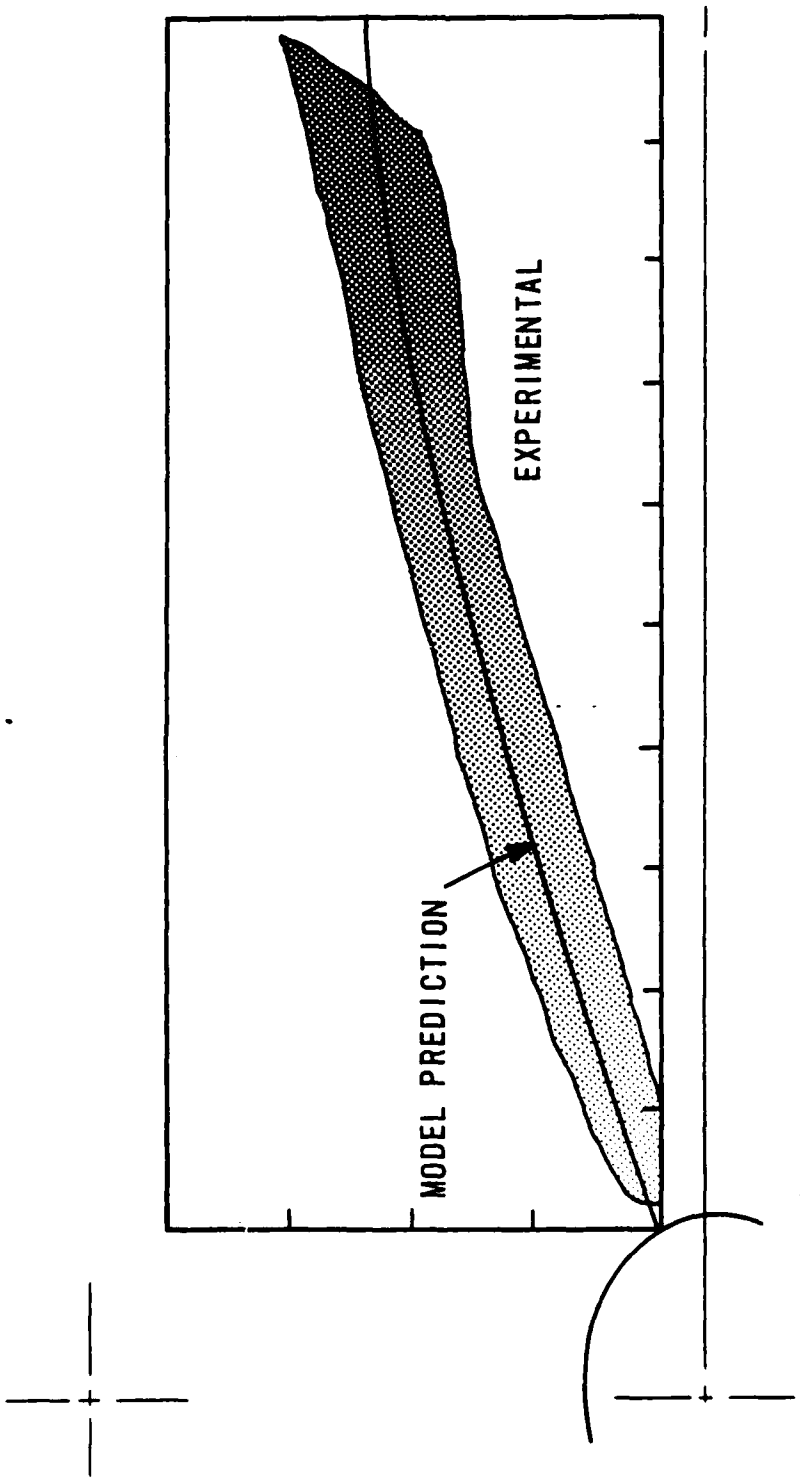

Figure 11. Model comparison to experiment with the bubble injection and $\dot{m}_{N_2}$ = 8.9 x 10^{-3} moles/

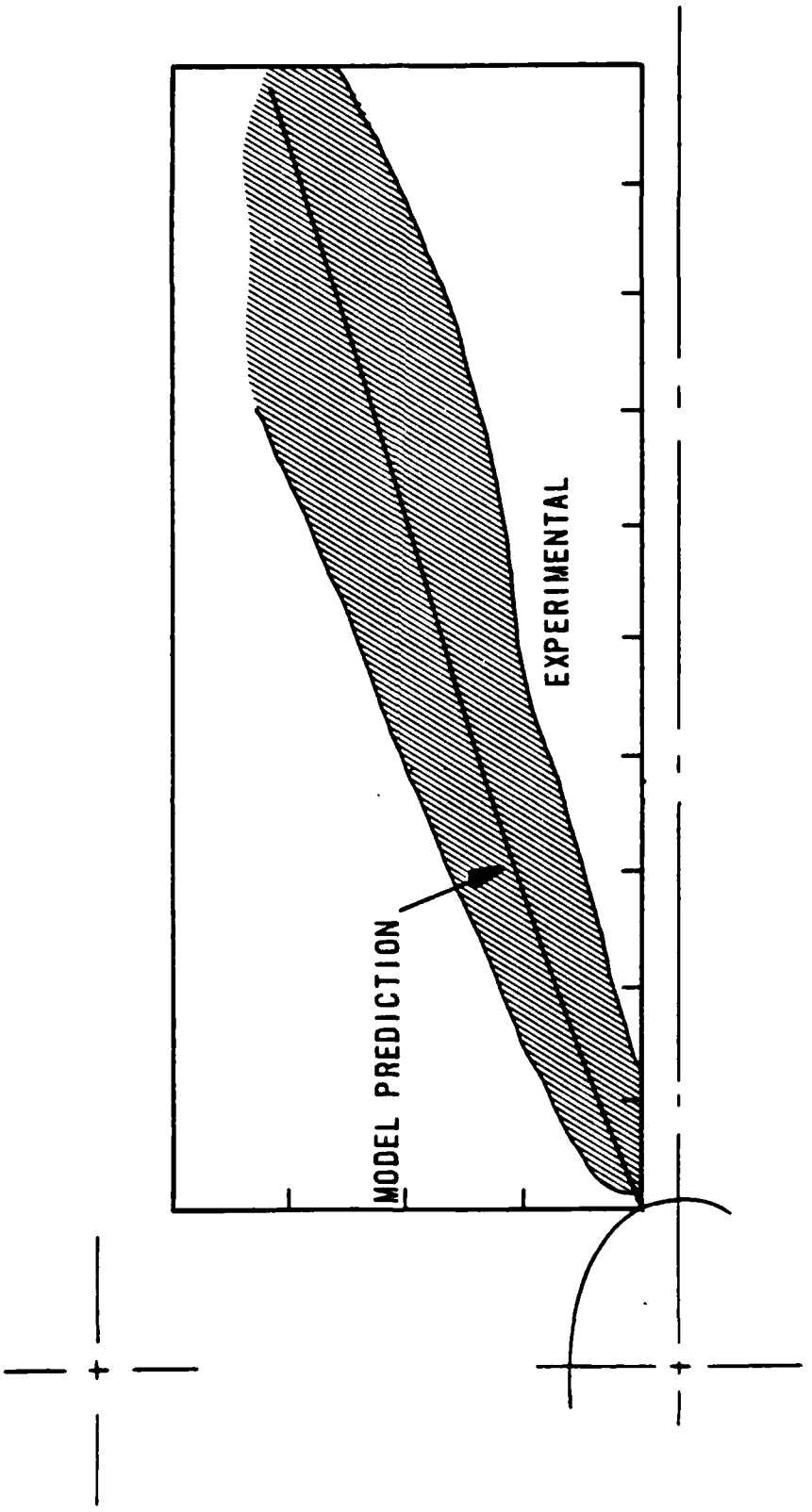

Figure 12. Model comparison to experiment with the 7 hole/injector and $\dot{m}_{N_2} = 3.52 \times 10^{-2}$ moles/s.

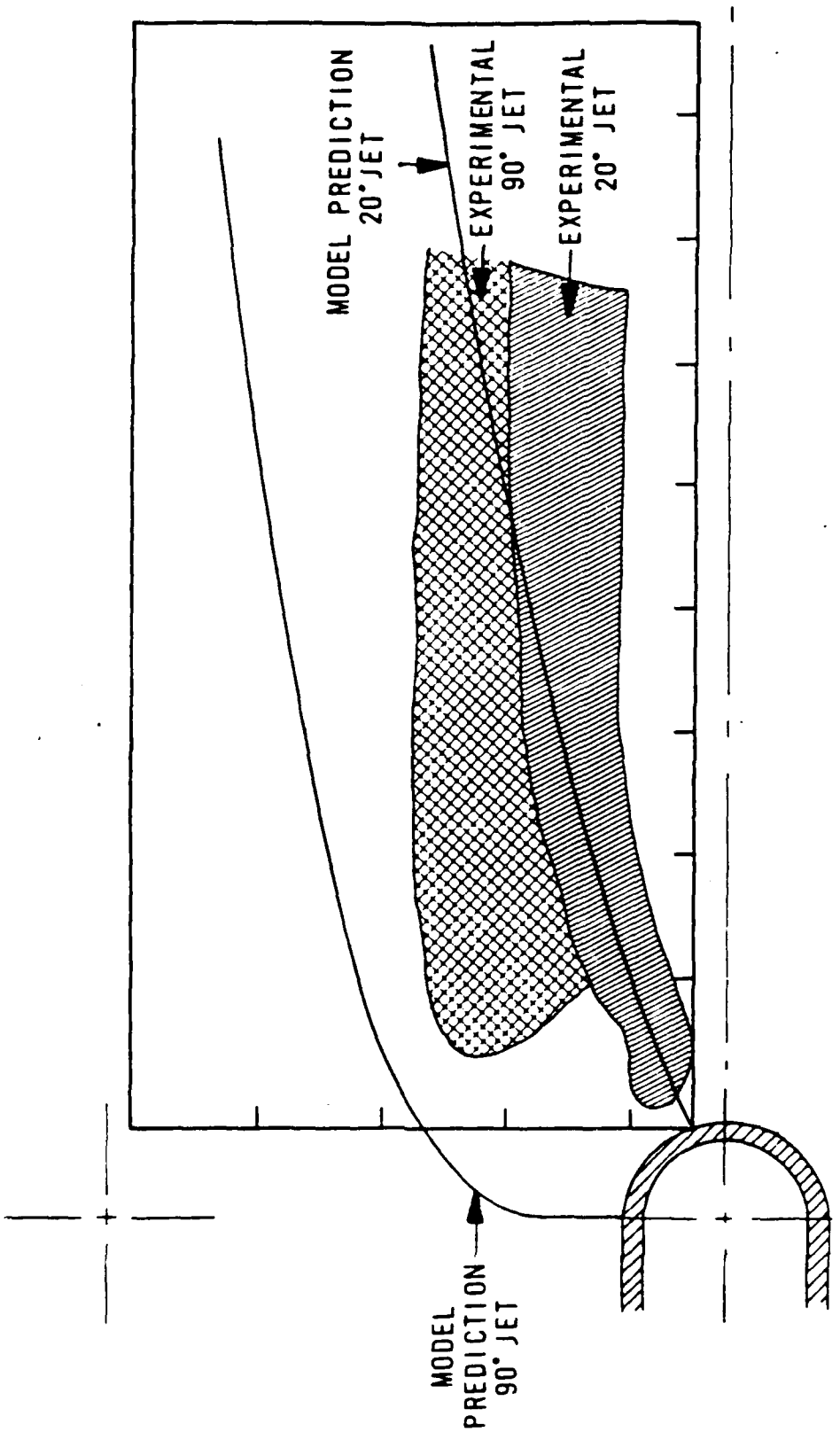

Figure 13. Model comparison to experiment with the 38 hole/injector and $\dot{m}_{He} = 3.52 \times 10^{-2}$ moles/s.

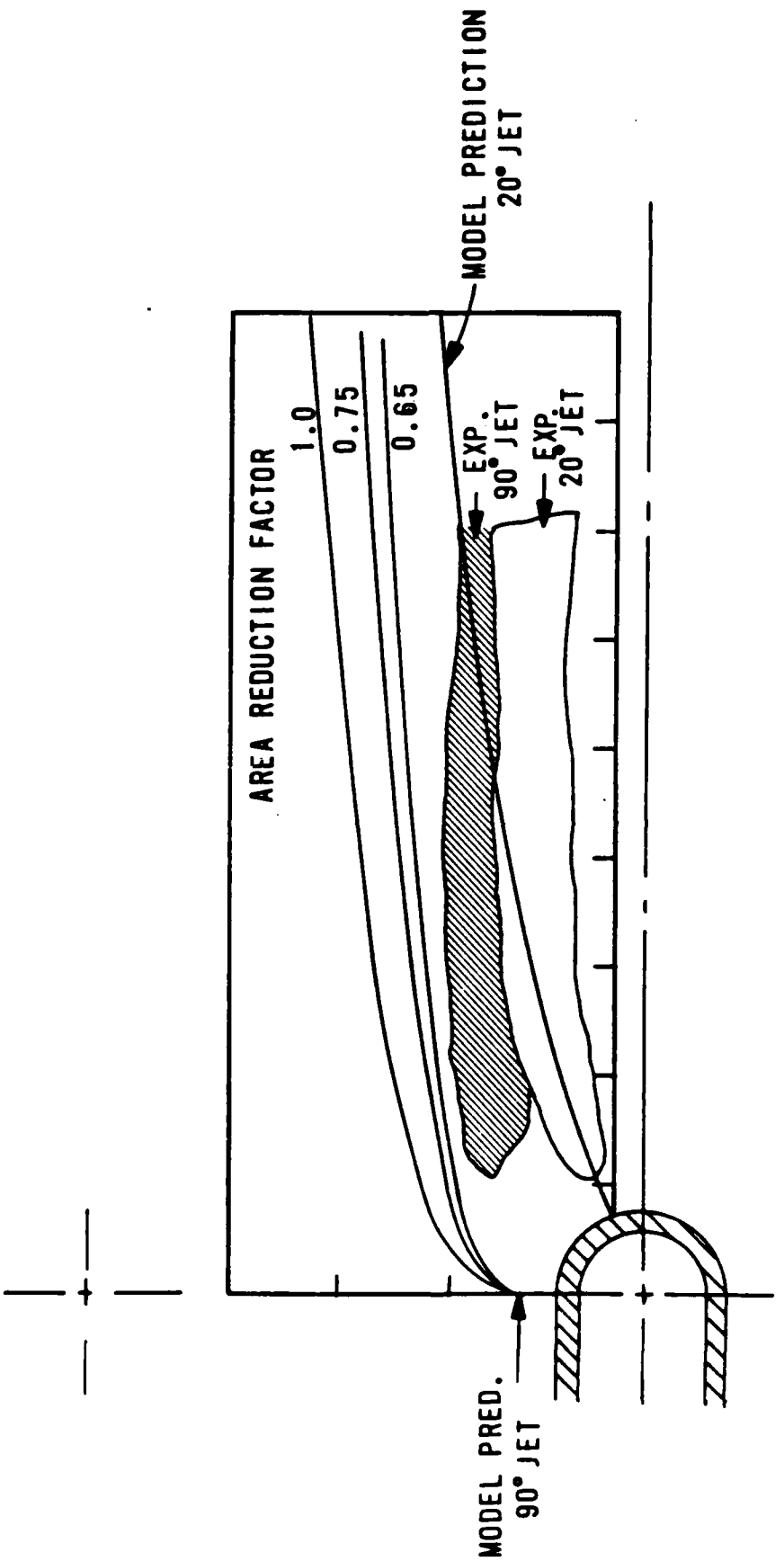

Figure 14. Effect of area blockage.

20 deg jet. For the 90 deg jet, neither the finite dimension of the channel spacing between injectors nor the blockage factor due to the jets themselves, causing an increase in primary dynamic pressure, have been included in the theoretical model. The latter effect can be seen in Figure 14 in which the primary area was arbitrarily reduced by an area reduction factor from 1.0 to 0.65. It is seen that the predicted jet penetration is significantly reduced with decreasing primary area. The area reduction factor can be roughly estimated by assuming the jets to act as solid cylinders of a diameter equal to the orifice diameter. A 0.75 area reduction factor will result if the perpendicular portion of the jet along the orifice centerline is 0.10 in. The best fit in the case shown was with an area reduction factor of 0.65 (Fig. 14). The 20 deg jet is influenced by this effect to a lesser extent (Fig. 14). In addition, there is evidence (Ref. 7) that multiple jets positioned side-by-side in close proximity (7.5D or less) will have their trajectories modified over that of a single jet, as was found in this case.

VI. CONCLUSION

The jet trajectory analysis is a quasi-empirical technique which follows the methodology presented by Shetz and Billig (Ref. 3) for gaseous jets. The fundamental assumption in the analysis is that the Ivanov jet trajectory correlation (Ref. 4) will be valid for underexpanded jets, to which the data corresponded, as well as pressure matched jets.

The comparisons of the jet centerline prediction and experimental outline of the jet plume as shown in Figures 11 to 14 illustrate a fairly good agreement with the experimental data. However, the least successful comparison occurred when the jet occupied a significant portion of the primary flow. Further refinements in the analysis will be required to account for jet/free stream interaction. That is, the jet trajectory analysis of Shetz was developed for a single jet exhausting into an infinite primary flow. The actual configuration consists of an array of jets exhausting in the flow in a confined channel. It is apparent, therefore, that there are regimes where the determination of the jet trajectory must be coupled with the effects of adjacent jets.

This was somewhat compensated for by implementing the area reduction factor. The model more closely reflects the interaction of the jets when this factor is incorporated. However, the use of the factor needs to be better quantified to be useful in predicting jet trajectories where experimental data is not available. Future work will be directed to such efforts.

The LIF method provides an excellent means for observing mixing in a laser cavity. The correlation of observed I_2 flow and mixing to the level of gain in the O_2-I laser allowed for correction of a major problem with the laser system. As previously noted, the trade-off between higher pressures in the $O_2(^1\Delta)$ generator and increased mixing had to be maximized for output power, since higher generator pressures cause greater $O_2(^1\Delta)$ deactivation. As a direct result of LIF tests and analysis, the device was updated with Nozzle No. 2 type injectors. Other slight modifications were also performed to improve

flow. The result of the improved mixing was that extractable power more than doubled. Higher gain was achievable with the improved mixing of Nozzle No. 2, as well as, increased power output.

We have presented a verifiable model for predicting jet trajectories in the case of underexpanded jets in a subsonic condition. It has also been demonstrated that LIF is an extremely useful tool for developing future refinements to trajectory models. Additional LIF studies should be performed by seeding the primary flow with I_2 and comparing results with that of the secondary flow jets. This work would allow for a determination of the mixing regime. Currently, work is being supported to study reactive flows to better understand mixing phenomenon in the presence of chemical reactions.

REFERENCES

1. Rapagnani, N. L. and Davis, S. J., "Laser-Induced I_2 Fluorescence Measurements in a Chemical Laser Flowfield", AIAA Journal, 17(12), pp. 1402-1404, December 1979.

2. Davis, S. J. and Hanko, L., Laser Digest-Spring 1979 , AFWL-TR-79-104, pp. 128-135, Air Force Weapons Laboratory, Kirtland Air Force Base, NM, July 1979.

3. Schetz, J. A. and Billig, F. S., "Penetration of Gaseous Jets Injected into a Supersonic Stream", J. Spacecraft and Rockets, 3(11), Nov 1966.

4. Abramovich, G. N., The Theory of Turbulent Jets, The MIT Press, Cambridge, MA, pp. 541-553, 1963.

5. Crist, S., Shevnan, P. M., and Glass, D. R., "Study of the Highly Underexpanded Sonic Jet", AIAA Journal, 4, pp. 68-71, January 1966.

6. Love, E. S., et al., Experimental and Theoretical Studies of Axisymmetric Free Jets, NASA-TR-R-6, Langley Research Center, Langley, Virginia, 1959.

7. Isaac, K. M. and Schetz, J. A., "Analysis of Multiple Jets in a Cross-Flow", ASME J. Fluid Engineering, 104, pp. 489-492, December 1982.

END

DATE

FILMED

FEB.

1988